ISSN: 0001-5113 AADRAY	ACTA ADRIAT., 47 (Suppl.): 185 - 206, 2006	UDC: 551.465(450)(262.3) 551.466(450)(262.3

A strong bora event in the Gulf of Trieste: a numerical study of wind driven circulation in stratified conditions with a pre-operational model

Alessandro CRISE [1*], Stefano QUERIN [1] and Vlado MALAČIČ [2]

[1] Istituto Nazionale di Oceanografia e di Geofisica Sperimentale (OGS), Borgo Grotta Gigante, 42/C, 34010 Sgonico (Trieste), Italy

[2] National Institute of Biology (NIB), Marine Biology Station, Fornače 41, 6330 Piran, Slovenia

**Corresponding author, e-mail: acrise@ogs.trieste.it*

This study investigates the circulation driven by a severe bora wind event in the Gulf of Trieste during the stratification season. A preliminary numerical analysis of the wind driven transport in the surface boundary layer is carried out for an idealized, laterally unbounded, shallow domain. Then, the simulations are focused on the Gulf of Trieste, using a realistic bathymetry and assuming stably stratified initial conditions. First, the model is driven by constant wind forcing, then qualitative and quantitative estimations of the dynamics of the basin are made reproducing the strong Bora event of the 25 June 2002. Numerical results show good agreement with in situ *measurements and remotely sensed images. The relevance of coastal upwelling and its persistence are also assessed. The results prove that mixing and coastal upwelling (both wind-driven) govern the circulation of the basin. When bora starts blowing, buoyant surface water is moved by EKMAN transport offshore inducing a bottom onshore current. Simultaneously, wind driven stirring breaks the initial stable stratification. The surface offshore current generates a sea surface level setup on the northern boundary. When bora decreases, this surface tilt is no longer sustained, and a reversal of the circulation is observed in the upper layer. The sensitivity to the wind forcing is also discussed. All of these issues are crucial to environmental problems such as pollutant dispersion or anoxia phenomena in the bottom layers of the Gulf.*

Key words: wind driven circulation, bora wind, EKMAN layer, upwelling, mixing

INTRODUCTION

The Gulf of Trieste (Fig. 1) is the northernmost part of the Adriatic Sea. Its circulation is driven by the interplay of different forcings: wind stress, buoyancy fluxes and remote control of the Adriatic Sea (i.e.: general circulation, tides, seiches). Many numerical studies have been carried out on the key processes and problems regarding the Gulf of Trieste. Researches on tidal dynamics (MOSETTI & MANCA, 1972; CAVALLINI, 1985; MALAČIČ *et al*., 2000), storm surge events (ACCERBONI & MANCA, 1973), dispersion of pollutants (OLIVO, 2002), convective processes (QUERIN, 2002, henceforth Q02), dispersion (in barotropic conditions) of radionu-

clides (LONGO *et al*., 1990) and oil spill events (CARMINATI *et al.,* 1994) provide a wide range of investigations on many relevant issues. However, a comprehensive numerical study on the dynamics of the Gulf of Trieste is still lacking. The goal of this modeling effort is to set up a model that is able to evaluate, to hindcast and eventually to predict the dynamics of this basin. The model, called ACOAST 1.1, is one of the high-end, nested (ZAVATARELLI & PINARDI, 2003) coastal models designed to fit the international ADRICOSM project requirements. Here we want to demonstrate the diagnostic capabilities of ACOAST 1.1 under severe wind forcing, starting from stratified initial conditions.

The simplified theory for the wind driven circulation proposed by EKMAN (1905) can hardly be applied to real cases, especially in coastal areas. When K_m (vertical eddy viscosity coefficient) varies in space (and time), analytical solutions (when they exist) depart from the EKMAN'S theory. Some attempts were carried out to obtain an explicit relation for the variation of K_m with depth (HUANG, 1979).

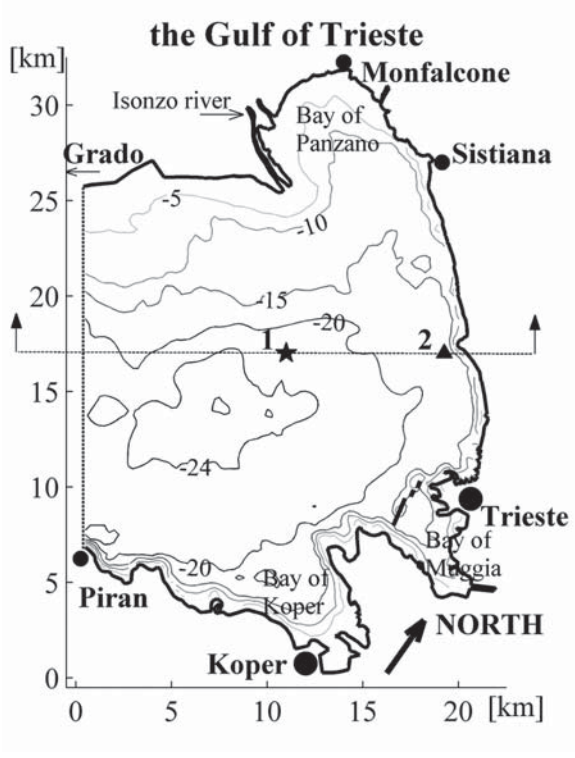

Fig. 1. Model domain: the Gulf of Trieste (rotated 30° clockwise). The 5, 10, 15 and 24 m isobaths are shown. The open boundary of the model is indicated by the dashed line between Grado and Piran. The center of the domain (point 1), the position of the MAMBO (OGS) meteomarine buoy (point 2) and the vertical section shown in Fig. 11 are also indicated

From the experimental point of view observations show that, when wind forcing lasts for a time equal or longer than the inertial period, the flow within the mixed layer is nearly depth independent: the mixed layer moves like a slab and the current shear is concentrated at the top of the thermocline (e.g.: SCHUDLICH & PRICE, 1998). Furthermore, both geostrophy and EKMAN transport produce the flow patterns that are observed in current measurements. However, only long time series can determine in a statistically significant way which of the two forcings is dominant (WELLER *et al*., 1991). Finally, the presence of lateral boundaries in enclosed or partially-enclosed basins can significantly modify the wind driven circulation (e.g.: winds blowing with a non negligible component favorably oriented along-shore cause coastal upwelling phenomena).

On the other hand, numerical simulations explicitly resolve the large scale processes parameterizing the small scale features with proper turbulence closure schemes. Hence, the numerical models are helpful tools for assessing the capabilities and the limits of simplified theoretical formulations.

In the actual configuration the ACOAST 1.1 model for the Gulf of Trieste explicitly simulates the large scale horizontal circulation (e.g.: EKMAN transport) and the vertical motions (e.g.: coastal upwelling), while parameterizes the so-called sub-grid turbulent motions through horizontal and vertical eddy coefficients. Since we aim at studying these processes at high resolution, we focus on events characterized by short time scales (few days).

First, the model is run on an idealized, double periodic (laterally unbounded) shallow domain and it is driven by constant and uniform wind forcing. The effects of stratification and of different parameterizations of vertical turbulent processes are analyzed, comparing the model output to the theoretical solution of the EKMAN

problem. Then, the role of a realistic bathymetry is shown using the same forcings of the previous ideal cases but considering the morphology of the Gulf of Trieste. Finally, the effects of a strong bora event, recorded in the 24 - 27 June 2002 period (Fig. 2), are investigated to appraise the wind influence on the general circulation of the basin and on the structure of the (initially stratified, Fig. 3) water column.

Bora is an ENE cold katabatic wind, stronger on the northeastern side of the Adriatic Sea. Its outbreaks are spatially influenced by the local topography and are characterized by a sudden startup and a short duration (order of one to a few days), with mean speed over 50 kmh^{-1} and with gusts largely greater than 100 kmh^{-1} (STRAVISI, 2001). Such Bora events, typical of the winter season, are not uncommon also in summer.

An introductive analysis of the June 2002 case study was carried out in Q02. A Large Eddy Simulation (LES) model was applied to a small scale (128×128×18 m), double periodic domain to reproduce wind driven mixing and convection. This simulation was able to properly reproduce the vertical mixing dynamics but failed in

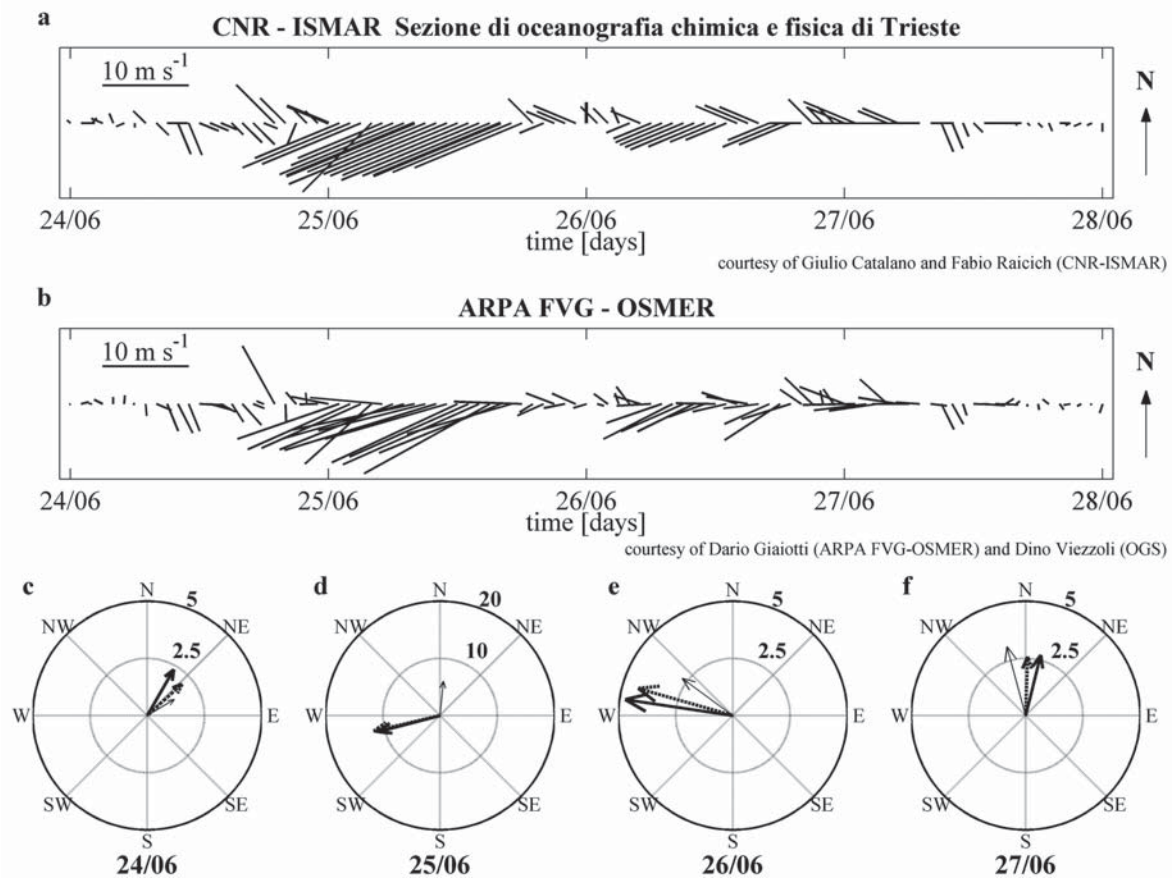

Fig. 2. Boundary conditions: wind speed (hourly means) measured by CNR-ISMAR (Sezione di oceanografia chimica e fisica di Trieste: (a) and by ARPA FVG - OSMER (OSservatorio MEteorologico Regionale: (b). Both meteorological stations are located in Trieste, near the coast. The prevalent wind (especially during the day of maximum intensity: 25 June 2002) is bora (blowing from ENE). Plots c, d, e and f show a comparison between the average wind forcing during the four days considered in the numerical simulations: thick line (CNR-ISMAR), dashed line (OSMER), thin line (MAMBO buoy). MAMBO buoy data are sampled every three hours and the meteorological station is sheltered by the local topography: this explains the remarkable differences with the other data sets. Wind measured by CNR-ISMAR is used as surface forcing for the simulations with realistic bathymetry and boundary conditions (run 6 and 7, see Table 1)

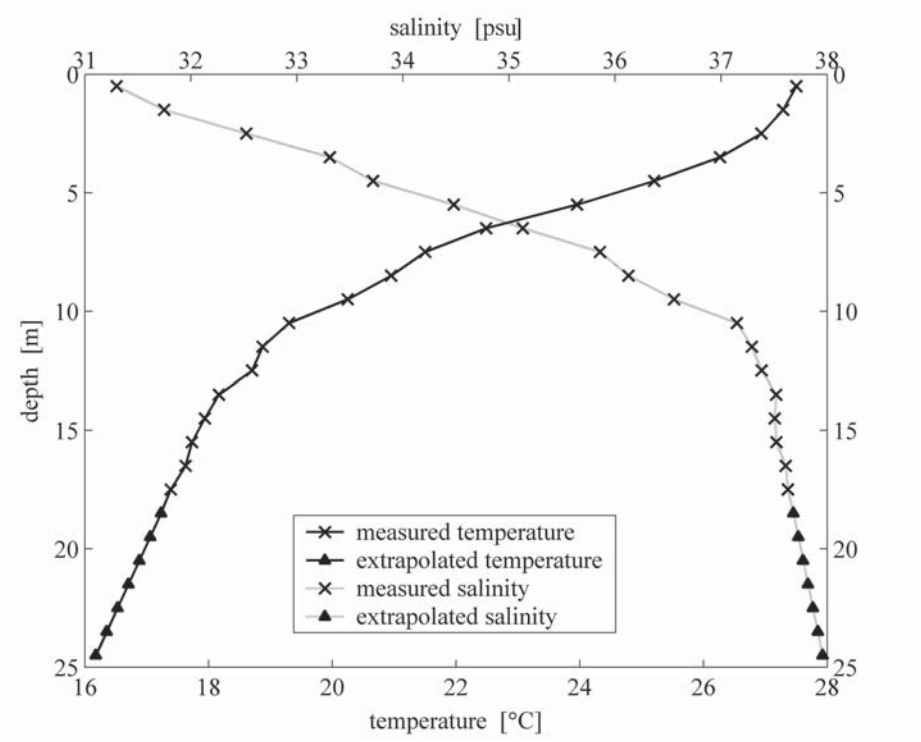

Fig. 3. Temperature and salinity initial conditions (24 June 2002, 00:00) for the numerical simulations, as measured by the MAMBO buoy. The last 7 values (18.5 to 24.5 m depth) are extrapolated linearly but reproduce fairly well the typical summer thermohaline profiles measured in the Gulf of Trieste

keeping temperature (T) and salinity (S) prediction within the measured range of T and S profiles. These profiles are automatically collected every 3 hours by a yo-yo CTD installed on the MAMBO (Monitoraggio AMBientale Operativo - OGS) buoy, deployed at 45° 41.86'N; 13° 42.51'E. The conclusion in Q02 was that coastal upwelling played a basic role in laterally advecting heat and salt, but the domain of the LES model (small scale, double periodic box) was unfit to take into account coastal interactions.

In this study we adopt a fully three-dimensional approach on a basin scale in order to reproduce not only the vertical, but also the lateral dynamics. As demonstrated in Q02, atmospheric buoyancy fluxes account for less than 10% of the temperature variability (negligible influence on the salinity) in the water column during the wind event. Therefore, in this particular case-study we assume adiabatic conditions at the air-sea interface in order to elicit the role of wind forcing.

The paper begins with a brief overview of the model, and then follows a description of the numerical simulations and their results. A comparison with an experimental data set gives a preliminary validation of the model output. Finally a conclusive comment on the main results is given together with an outlook on future work.

THEORETICAL BACKGROUND

Wind driven circulation in coastal areas is obtained as a superposition of the direct (EKMAN) effect on the surface layer and the horizontal pressure gradient induced by the presence of a coastal boundary. The pressure term can be split into a baroclinic and a barotropic component. In the case under study, a simple scale analysis suggests that, in the surface layer, the velocity obtained by the density driven pressure gradient can be neglected as long as the wind is blowing. The steady-state, linear EKMAN equations read:

$$-fv = -\frac{1}{\rho}\frac{\partial p}{\partial x} + (\nu + K_m)\frac{\partial^2 u}{\partial z^2}$$

$$fu = -\frac{1}{\rho}\frac{\partial p}{\partial y} + (\nu + K_m)\frac{\partial^2 v}{\partial z^2}$$

where f stands for the CORIOLIS parameter, u and v for the zonal and the meridional component of velocity, p for pressure, ρ for density, ν for the kinematic viscosity coefficient and K_m for the vertical eddy viscosity coefficient.

Surface boundary conditions are given by:

$$\rho\nu\frac{\partial u}{\partial z} = \tau_x \ , \ \rho\nu\frac{\partial v}{\partial z} = \tau_y$$

where τ_x and τ_y are the three components of the wind stress. The ocean interior is assumed to be in geostrophic equilibrium.

The general solution can be mathematically obtained by the superposition of a homogeneous (purely EKMAN) and a non-homogeneous (pressure dependent) equation. We will see that the barotropic component of the pressure term is the dominant one in the presence of wind stress. The magnitude of the pressure gradient term is determined by the maximum between the barotropic and baroclinic term, namely:

$$O\left[\frac{\partial p}{\partial x}\right] = g\left\{O\left[\frac{\Delta}{\Delta x}(\rho(x)\cdot\eta(x))\right]\right\}$$
$$= g\,\mathrm{MAX}\left\{O\left[\frac{\Delta\rho}{\Delta x}\eta\right], O\left[\frac{\Delta\eta}{\Delta x}\rho\right]\right\}$$

where g is the acceleration due to gravity and η is the sea surface elevation.

The typical scales of the Gulf of Trieste (derived from experimental observations) are $\Delta\rho = O(1)$ kgm^{-3}, $\Delta x = O(10^4)$ m, $\Delta\eta = O(10^{-2})$ m, $\eta = O(10^{-1})$ m, $\rho = O(10^3)$ kgm^{-3}, hence:

$$O\left[\frac{\partial p}{\partial x}\right] = g\,\mathrm{MAX}\left\{O\left[\frac{1}{10^4}10^{-1}\right], O\left[\frac{10^{-2}}{10^4}10^3\right]\right\}\ \mathrm{kg\,m^{-3}}$$
$$= O\left[10^{-2}\right]\mathrm{kg\,m^{-3}}$$

When the wind driven currents raise the sea level, the barotropic pressure gradient is the dominant term. Under steady state conditions and in the presence of a laterally bounded domain however, the pressure gradient force along the sea surface slope is balanced by the wind stress component acting in the opposite direction. Only the wind stress component orthogonal to the surface slope conveys momentum and energy into the ocean.

THE NUMERICAL MODEL

The model is based on the modular structure of the MITgcm (Massachusetts Institute of Technology general circulation model) code, developed at MIT, Boston. The code, in the beginning, was designed for deep convection studies in the open ocean (as an overview, see MARSHALL *et al*., 1997; MARSHALL & SCHOTT, 1999), yet its applicability was then broadened to simulations with large scale variability (from a few meters scale, up to global circulation problems), for both hydrodynamic and atmospheric applications. The most important features of the MITgcm numerical model are specified as follows:

- it is a finite volume, free surface model;
- it can be used to study problems for which the hydrostatic approximation does not hold;
- the vertical discretization is obtained using *z*-levels with partial cells;
- it uses a semi-implicit time stepping, without mode splitting;
- it allows the use of alternative numerical schemes for the advective and diffusive terms;
- it is a RANS (REYNOLDS Average NAVIER-STOKES equation) model: the turbulence closure for the horizontal component is achieved with constant harmonic and bi-harmonic coefficients of eddy viscosity and diffusivity;
- the vertical processes of mixing and diffusion can be parameterized either with constant harmonic operators, or by the turbulence closure based on the KPP method (K-Profile Parameterization, LARGE *et al*., 1994);
- it is designed to ensure efficient portability on several computational platforms;
- it can be run in parallel mode using standard MPI (Message Passing Interface) calls.

The equations

The model solves the following set of equations for an incompressible fluid:

$$\frac{Du}{Dt} - fv + \frac{1}{\rho_c}\frac{\partial p}{\partial x} = F_u$$

$$\frac{Dv}{Dt} + fu + \frac{1}{\rho_c}\frac{\partial p}{\partial y} = F_v \qquad \text{(momentum equations)}$$

$$\varepsilon_{nh}\frac{Dw}{Dt} + g\frac{\rho}{\rho_c} + \frac{1}{\rho_c}\frac{\partial p}{\partial z} = \varepsilon_{nh}F_w$$

$$\frac{\partial u}{\partial x} + \frac{\partial v}{\partial y} + \frac{\partial w}{\partial z} = 0 \qquad \text{(continuity equation)}$$

$$\rho = \rho(\theta, S) \qquad \text{(equation of state)}$$

$$\frac{D\theta}{Dt} = Q_\theta \qquad \text{(heat equation)}$$

$$\frac{DS}{Dt} = Q_S \qquad \text{(salt equation)}$$

where F_u, F_v, and F_w stand for the three components of the external forces and of the dissipation term ($v\nabla^2\vec{v}$), ρ_c for the constant reference density, w for the vertical component of velocity and Q_θ and Q_S for the heat and salt fluxes. ε_{nh} is a non-hydrostaticity parameter, and can be set to 1 or 0 to obtain the full non-hydrostatic equation or to adopt the hydrostatic approximation, respectively. D is the substantial derivative operator.

Numerical implementation

The model domain is discretized on a cartesian ARAKAWA C grid, with a horizontal resolution of 250 m and a vertical resolution of 1 meter. The time step is 10 s.

The idealized simulations are run on a regular domain, with 64×64 cells in the horizontal direction and 25 levels in the vertical direction. The bottom is flat, 25 meters deep, and the 4 vertical boundaries are open (double periodic domain).

The grid for the Gulf of Trieste experiments is comprised of 88×128 cells in the horizontal direction and 25 levels in the vertical direction. The bathymetry is obtained from maritime charts by kriging interpolation and is rotated 30° clockwise in order to obtain a better fit in the grid space. The only open boundary (the imaginary vertical plane between Grado and Piran, Fig. 1) is on the western side of the domain.

The model uses a free surface formulation so as to solve the external gravity waves. An implicit solver of the linearized formulation of the free surface is employed, in order to keep the same time discretization for both the barotropic and the baroclinic mode. The numerical schemes implemented in the code are quasi-second order ADAMS-BASHFORT for time integration, centered difference for horizontal diffusion and advection and backward-implicit for vertical diffusion of both momentum and tracers.

The turbulence closure

As specified previously, the vertical mixing processes can be resolved using either constant viscosity and diffusivity coefficients or the KPP algorithm. This turbulence closure method is based on a two-equation model and parametrizes in a different way the ocean interior and the surface boundary layer. In particular, for the surface layer, the model evaluates its thickness which is the minimum depth at which the bulk RICHARDSON number exceeds a critical value (in this case: $\mathrm{Ri_{Bc}} = 0.3$). The mixing processes due to wind stress, surface fluxes (buoyancy and mass) and convective instability are solved using the following parameterization of eddy viscosity and of the double diffusion:

$$\overline{w'v'} = -K_m\left(\frac{\partial \bar{v}}{\partial z}\right)$$

$$\overline{w'\theta'} = -K_\theta\left(\frac{\partial \bar{\theta}}{\partial z} + \gamma_\theta\right)$$

$$\overline{w'S'} = -K_S\left(\frac{\partial \bar{S}}{\partial z} + \gamma_s\right)$$

$$K_i(\sigma = h/h_b) = h_b\, w_i(\sigma)\, G(\sigma)$$

where K_m is the eddy viscosity, K_θ and K_S are the eddy diffusivities, γ_θ and γ_S are the two terms related to the non-local transport, σ is the non-dimensional depth, h_b is the boundary layer thickness, w_i is the turbulent velocity scale and G is the polynomial shape function. The primed terms are related to the turbulent fluctuations of each quantity. Overbars denote the time averages.

The processes that involve the ocean interior (shear instability mixing, internal wave mixing, double diffusion phenomena) are parameterized using eddy viscosity and diffusivities which are functions of the gradient RICHARDSON number and the double diffusion density ratio.

Layout of the numerical experiments

The simulations are carried out assuming a constant CORIOLIS parameter (f-plane approximation), with a typical mid-latitude value ($f = 10^{-4} s^{-1}$), and an adiabatic forcing due to the wind stress only. All numerical experiments (see Tab. 1, as a summary) are run on the parallel IBM SP4 supercomputer installed at CINECA (Bologna, Italy), exploiting the parallelism through a domain decomposition of 2×2 equal size subdomains. The parallel communication protocol implemented in the model is MPI.

Initial conditions

The initial velocity field is null in all the simulations. The initial thermohaline conditions are either homogeneous (22°C, 36 psu) or stratified. The T and S profiles (Fig. 3) used in the stratified case studies (run 1, 3, 5, 6, 7, Table 1) are laterally homogeneous and are derived from the MAMBO buoy CTD data measured one day prior the onset of the bora event. The adjustment of the profile (only 17 m deep) to greater depths is made, when needed, by extending linearly the deepest values of temperature and salinity down to the bottom. This extrapolated vertical structure closely resembles the experimental profiles obtained by NIB-MBS (National Institute of Biology, Marine Biology Station, Piran) and LBM (Laboratorio di Biologia Marina, Trieste) in the deepest areas of the Gulf during the same period of the year in 2003. The quiescent initial conditions and the lateral homogeneity ensure that there is no available potential energy at the beginning of the simulations and all the work has to be done by the external forcings (i.e.: the wind).

The bulk non-hydrostatic number (KANTHA & CLAYSON, 2000), is defined as:

$$N_h = U/(L \cdot N)$$

Table 1. List of the simulations discussed in the text with their principal features

run	domain	OBCs	wind regime	turbulence parametrization	initial conditions T(z), S(z)
1	flat bottom box 25 m depth	double periodic	uniform and constant bora (14 ms^{-1})	constant eddy coefficients	MAMBO profile
2	flat bottom box 25 m depth	double periodic	uniform and constant bora (14 ms^{-1})	constant eddy coefficients	homogeneous (22°C, 36 psu)
3	flat bottom box 25 m depth	double periodic	uniform and constant bora (14 ms^{-1})	KPP profile	MAMBO profile
4	flat bottom box 25 m depth	double periodic	uniform and constant bora (14 ms^{-1})	KPP profile	homogeneous (22°C, 36 psu)
5	Gulf of Trieste	ORLANSKI radiation condition	uniform and constant bora (14 ms^{-1})	KPP profile	MAMBO profile
6	Gulf of Trieste	ORLANSKI radiation condition	measured bora (spatially uniform)	KPP profile	MAMBO profile
7	Gulf of Trieste	ORLANSKI radiation condition	measured bora (increased 30%, spatially uniform)	KPP profile	MAMBO profile

where U and L are the typical speed and length scales and N represents the BRUNT-VÄISÄLÄ frequency. In our case N_h is much less than one ($U = 10^{-1}m^{-1}$, $L = 2 \cdot 10^4$, $N = 2 \cdot 10^{-3}$, $N_h = 2.5 \cdot 10^{-3}$) on average but when strong wind blows and a vigorous upwelling takes place, the deep water outcrops and wind driven stirring breaks the initial stable stratification and (N_h tends to zero) and N_h assumes large values. In the realistic case-studies (realistic bathymetry, measured wind forcing) we used non-hydrostatic conditions to ensure numerical stability and accuracy of the results. Conversely, the idealized simulations are run using the hydrostatic approximation.

Boundary conditions

Surface boundary conditions

The model evaluates wind stress from wind velocity data using standard bulk formulae (LARGE & POND, 1981, 1982).

The simulations in idealized wind conditions (run 1-5, Table 1) are obtained using constant and uniform wind, blowing from the ENE (bora).

For the realistic case studies (run 6-7, Table 1), we used hourly mean wind forcing, spatially homogeneous over the basin. The meteorological data used in run 6 and 7 were measured by CNR–ISMAR (Consiglio Nazionale delle Ricerche – Istituto di Scienze MARine - Sezione di oceanografia chimica e fisica di Trieste). A comparison between these data and those measured by ARPA FVG–OSMER (Agenzia Regionale per la Protezione dell'Ambiente del Friuli Venezia Giulia – OSservatorio MEteorologico Regionale) and by OGS (meteomarine station installed on the MAMBO buoy) was also made (Fig. 2 c, d, e and f). The meteorological stations of the first two institutes are located in Trieste and produced similar data sets in the analyzed time period (Fig. 2 a and b). On the other hand, the data measured by the MAMBO buoy were obtained using a time averaging interval (3 hours) that, during periods with light winds, produced fairly reliable data although during the bora event provided velocities and directions inconsistent with the other stations. It must be pointed out that the MAMBO buoy is positioned very close to the shore in an area sheltered from the wind by the local topography (Fig. 1). Thus, the difference between the land and the buoy station data must be ascribed to both the sampling method and the geographic position.

Moreover, it is known that the bora wind is not spatially uniform over the northern Adriatic Sea and over the Gulf of Trieste. This katabatic wind is, in fact, strongly influenced by the local topography, characterized by the inland karstic plateau and the steep cliffs shoreward. The assumption of spatial homogeneity is a rather rough approximation for wind stress. Furthermore, the data measured in Trieste are influenced by the presence of buildings and represent a situation which is supposed to be quite different from the one that can be encountered in the center of the Gulf. At the moment, the results obtained by imposing homogeneous wind forcing are acceptable although in order to have a more realistic model configuration, coupling with a high resolution LAM (Limited Area Model) atmospheric model is in progress.

Lateral and bottom boundary conditions

The test cases with the idealized domain (run 1-4) are obtained using periodic conditions on the lateral boundaries (open ocean), as indicated in Table 1.

On the contrary, for the simulations with realistic bathymetry (run 5-7), the ORLANSKI radiation condition (ORLANSKI, 1976) for momentum and tracers is applied to the western open boundary (passive open boundary condition). Physical variables (velocity, temperature and salinity) at the boundary cells are thus governed by the following radiation equation:

$$(\partial\varphi/\partial t) + C\varphi_x = 0$$

where φ is any variable and C is the phase velocity of the perturbations originating inside the domain.

No flux conditions (for both momentum and tracers) and no slip conditions are imposed on the lateral solid boundaries.

As regards the bottom boundary, no slip

conditions are imposed for all 7 runs.

RESULTS AND DISCUSSION

This section is divided into two main subsections: the first describes the simulations run in idealized conditions while the second refers to the realistic case studies.

Simulations in ideal conditions

Numerical experiments firstly addressed a sensitivity analysis when running the full primitive equation model in an idealized configuration (constant and homogeneous wind stress, double periodic domain, with/without stratified thermohaline initial conditions) assuming different formulations of vertical eddy viscosity and diffusivity coefficients (next subsection, run 1-4 of Table 1).

In the following subsection (run 5 of Table 1) we analyze the vertical distribution of velocity by imposing the same wind forcing of run 1-4 but using the realistic bathymetry of the Gulf of Trieste as the domain.

Some comparisons with the analytical solution of the surface boundary layer equations (page 189) are made to assess the limits of the EKMAN theory of wind driven transport.

Ideal domain, ideal wind forcing case studies (run 1-4)

In the four idealized case studies we use the simple box-shaped domain described in on page 190 (64×64 grid cells of dimension 250 × 250 m, with constant depth – 25 m). A comparison with the analytical EKMAN solution was made to discriminate the effects of stratification and turbulence parameterization. The stratification, if present, is the same as the one adopted in the simulations run using the realistic bathymetry (Fig. 3).

If we impose constant eddy viscosity (run 1 and 2, Table 1), the time average of the numerical results perfectly reproduces the analytical solution of the EKMAN equation for the two horizontal components of velocity. The averaging procedure is necessary in order to filter out the inertial oscillations. In this case, as expected, the accuracy of the fit does not depend on stratification. (Fig. 4, plot a).

When the KPP algorithm is used, the velocity field is remarkably different: even if a spiral-like profile is maintained (Fig. 4 b and c), a direct comparison of the results (Fig. 4 d) shows that the flow is much less energetic.

Real domain, ideal wind forcing case study (run 5)

The same wind forcing of runs 1-4 is used also for run 5. In this latter case, the domain is the Gulf of Trieste and the simulation starts from stratified initial conditions. Fig. 5 shows the polar graphs of the horizontal velocity computed after one day of uniform bora wind forcing, when the velocity field becomes steady. Two sites are considered in order to appraise the differences in the vertical profile of velocity going from the offshore to the coastal areas: one (Fig. 5 a) is in the center of the basin (point 1 in Fig. 1, 24 m depth) while the other (Fig. 5 b) is at the same location as the MAMBO buoy mooring (point 2, 18 m depth). In the center of the basin, surface velocity vectors are oriented toward the western quadrant but the CORIOLIS force veers them to the right by about 30° with respect to the wind stress. At deeper levels, it is difficult to identify a spiral structure for the velocity profile, even if speed decreases and changes direction. In the deepest, 5 meter thick layer, the onshore current is almost totally driven by coastal upwelling. This is reflected in the kinetic energy (per unit mass) budget at 2, 10 and 15 m depth: $KE_{2m} = 5.19 \cdot 10^{-3}$ m^2s^{-2}, $KE_{10m} = 1.11 \cdot 10^{-3}$ m^2s^{-2} and $KE_{15m} = 5.08 \cdot 10^{-3}$ m^2s^{-2}. The wind driven surface offshore current is balanced by an onshore inflow in the bottom layer. This explains the KE minimum found at 10 m depth, where the velocity inverts its direction.

The surface velocity in the coastal area is approximately parallel to the wind stress, both in transient and steady state conditions. We focus on the steady state condition: a LAGRANGIAN approach can explain this apparent anomaly. A dynamical equilibrium keeps the mass balance near the coast as the water parcel is pumped

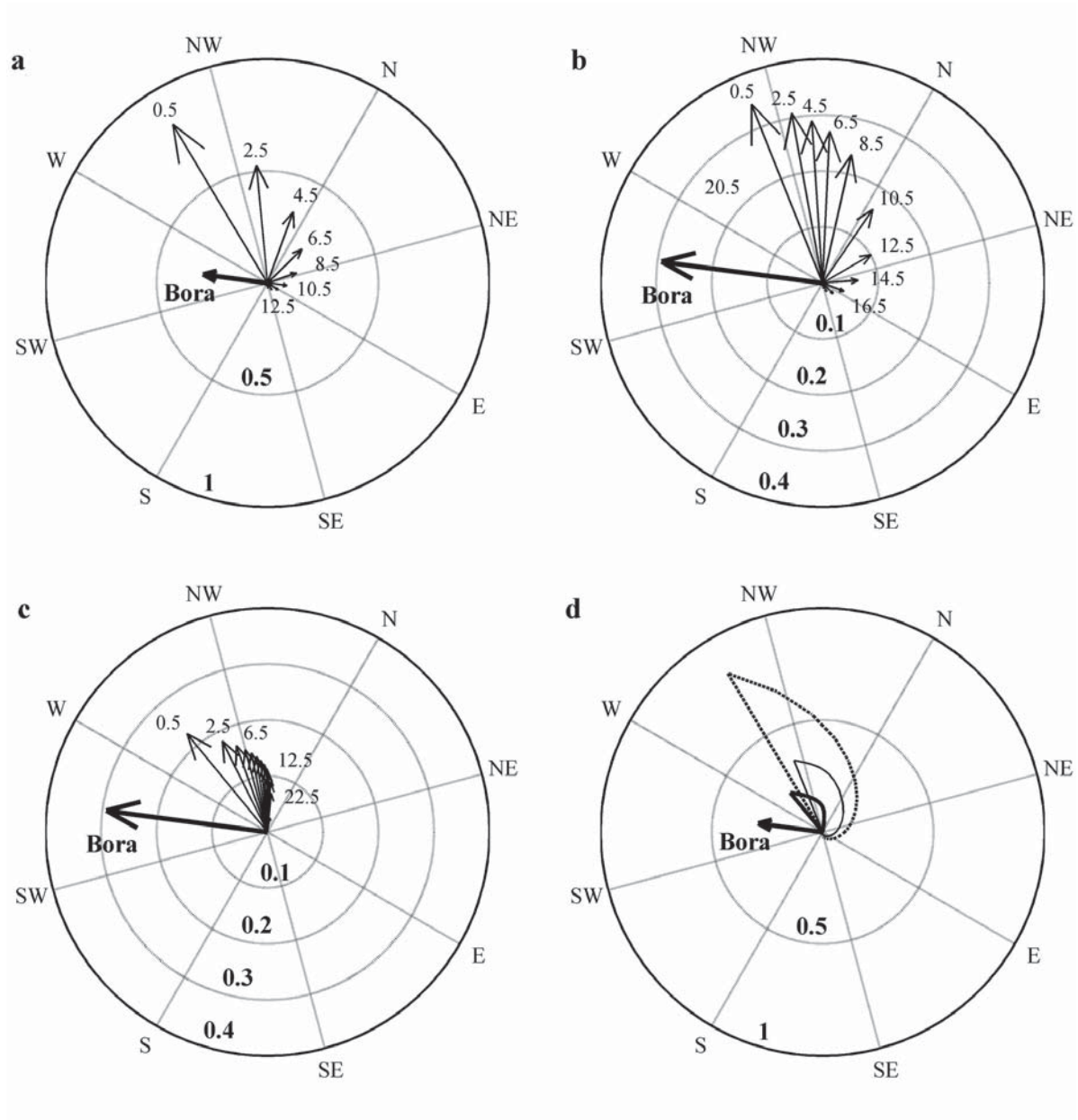

Fig. 4. Comparison between EKMAN'S theory and model results: polar graphs of the time averaged horizontal components of velocity at increasing depth. To obtain clearer pictures, vectors are presented every 2 m. Wind stress (constant and uniform bora (ENE), after a spin-up period in which wind velocity increases from 0 to 14 ms^{-1} - 0.292 Pa) is represented by the bold vector. The orientation of the polar plot (30°) is coherent with the orientation of the model grid used for the realistic case studies. The model domain is an ideal box, with periodic lateral boundary conditions (open ocean configuration) and flat bottom. Plot a shows model results obtained using constant vertical eddy viscosity coefficients (run 1 and 2, Table 1): the numerical solution is identical to the analytical EKMAN spiral. Velocity fields are also insensitive to stratification: the three cases (analytical, numerical stratified, numerical non-stratified) can be superimposed. Plots b and c are obtained by adopting the KPP algorithm but starting from stratified (see Fig. 3) and homogeneous (22°C, 36 psu) initial thermohaline conditions, respectively. A direct comparison of the three solutions is shown in plot d: EKMAN spiral (dashed line), KPP-stratified case (thin line), KPP-homogeneous case (thick line)

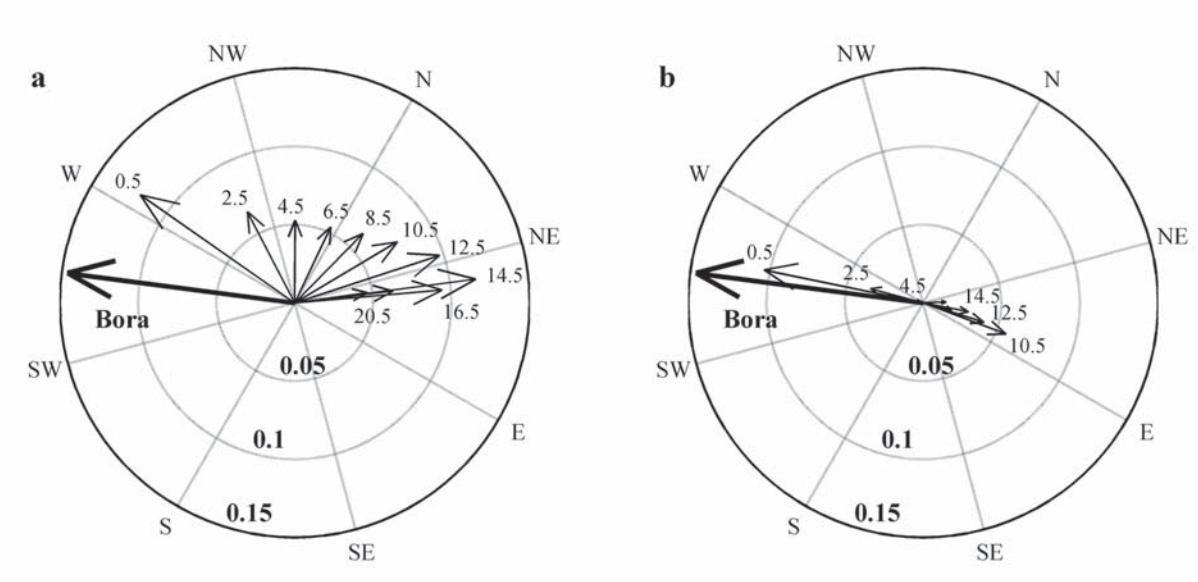

Fig. 5. Polar graphs of horizontal components of velocity at increasing depth. To obtain clearer pictures, vectors are presented every 2 m. Plots are obtained using the same conditions as Fig. 4, plot b (uniform and constant wind, KPP turbulence parametrization, stratified initial conditions), except for the domain, in this case the realistic bathymetry of the Gulf of Trieste. Velocity fields are sampled in point 1 (center of the basin, 22 m depth, plot a) and point 2 (coastal area, 18 m depth, plot b) shown in Fig. 1. The spiral-like behaviour of the velocity field is no longer reproduced (especially in coastal area, where the effect of the bathymetry is dominant, plot b)

upwards by the wind stress and subsequently takes its direction. Only off-shore does the CORIOLIS adjustment modify the direction of motion. Near the eastern boundary the velocity of a water parcel is low compared to the surface layer velocity. Below the upper EKMAN layer the parcel slowly rises along the coast and when it enters the surface layer, it suddenly accelerates horizontally because of the steady wind stress. From a LAGRANGIAN point of view, the wind starts at that moment ($t = 0$). The parcel trajectory can be described by the analytical solution of the time-dependent Ekman flow equations: this solution is represented by the Cornu spiral in the hodogram ($x(t)$, $y(t)$) plot (HASSELMANN, 1970; KANTHA & CLAYSON, 2000). The derivative of the solution (i.e. the velocity) can be expressed as a trigonometric tangent function. When the water parcel reaches the surface ($t = 0$) the tangent is null: this means that the parcel velocity and the wind stress are parallel.

Assuming the averaged eddy viscosity coefficient in the upper layer:

$$\langle K_m \rangle = 9.6 \cdot 10^{-3}\,\mathrm{m^2 s^{-1}}$$

the EKMAN vertical scale D_E is:

$$D_E = \left(\frac{2\langle K_m \rangle}{f} \right)^{1/2} = O[10m]$$

which is high, if compared to the vertical length scale of the velocity decay at both positions. These results further demonstrate that the EKMAN theoretical analysis must be applied carefully to real case studies, especially in shallow embayments.

The June 2002 bora event (run 6-7)

The last two numerical experiments are devoted to analysis of the circulation with realistic domain and boundary conditions using time-varying measured wind forcings. A non-negligible contribution to the circulation is given by the surface currents that originate when wind stress no longer sustains the wind set-up. Even if the runs simulate a 4 day time period (from 00:00 of 24 June to 00:00 of 28

June 2002), we focus our attention in particular on the day of maximum wind stress (25 June, Fig. 2).

The case study has been selected in such a way that wind stress is the dominant forcing, to reduce as much as possible the importance of the other factors (buoyancy fluxes, river input, remote forcing of the northern Adriatic Sea). At the beginning of the event, the stratification is well developed, as shown in Fig. 3.

A preliminary assessment of surface heat fluxes can be made to justify the adiabatic assumption in the model configuration. The heat flux data, calculated using the bulk formulae derived by PICCO (1991), were kindly provided by CNR-ISMAR. The data show that the basin gains heat in the period 24-27/06/2002 (average heat flux: +105 Wm^{-2}), while there is a net heat loss during the period 00:00 – 18:00 of 25/06/2002 (-134 Wm^{-2}) when bora is very intense and induces a strong negative latent heat flux due to evaporation. So, the adiabatic hypothesis roughly holds, at least during the first 2 days of the simulation.

River runoff, not yet considered by the model, is known to form a buoyancy gradient that induces a freshwater plume and a wedge-like coastal current exiting the Gulf. This flux is balanced by an incoming current along the Istrian coast. In summer, however, the river buoyancy input is negligible (few tenths of m^3s^{-1}).

The remote forcing induced by the northern Adriatic Sea is also neglected and the ORLANSKI radiative boundary condition is applied to the open boundary of the model.

Comparison with experimental data

In this subsection, the numerical results are compared with experimental data. The temperature and salinity vertical profiles and the sea surface temperature (SST) maps are compared to the MAMBO buoy CTD data and with satellite infrared images, respectively.

Fig. 6 shows the MAMBO data and the model results: the upwelling event caused by the sudden outbreak of bora wind is clearly reproduced by the model. The initial stable temperature stratification is suddenly broken and, at 12:00 on 25 June, the water column is almost homogeneous (17.5 °C at the bottom and 19 °C at the surface). Salinity shows similar behavior. Since the model is adiabatic, the effect of heat fluxes at the surface is neglected. For example, surface heating during the day (measured by the buoy and visible in Fig. 6a) cannot be reproduced by the model. The acceptable resemblance between the experimental data and the numerical results proves that the strong cooling during wind events is mainly due to mechanical interactions, rather than heat fluxes. In particular, the wind driven mixing acts over the entire basin while the upwelling phenomenon affects only the coastal areas, where the wind driven water depletion pumps dense water from the bottom layers.

The satellite SST data and the model results also show good agreement. Figs. 7 and 8 compare the satellite SST maps (on the left) and the model output (on the right) before and after the bora event. The AVHRR data coming from the NOAA 12 and the NOAA 16 satellites have an accuracy range of ±0.5 °C (NOTARSTEFANO *et al*., 2004). On 24 June, the surface temperature is very high and uniform over the entire basin (Fig. 7). The cold spots near the coast in the Bay of Panzano and the Bay of Koper are most likely due to the discharge of the rivers, and neglected by the model. Fig. 8 shows the effect of the bora wind. The surface temperature decrease is up to 10 °C in the southeastern area of the basin, where the upwelling takes place. The temperature pattern is well reproduced by the model, even if there are some differences in the temperature values. In particular, there is an important discrepancy that is confined to the north-western coastal area of the Gulf and in the Bay of Panzano. This discrepancy can be ascribed to the river input, the forcing at the open boundary and the heat fluxes (all neglected in the model configuration).

The effect of the heat forcing in that area (characterized by a very shallow bathymetry, if compared with the rest of the domain) can be roughly estimated using simple considerations. Experimental data show that, from the onset of

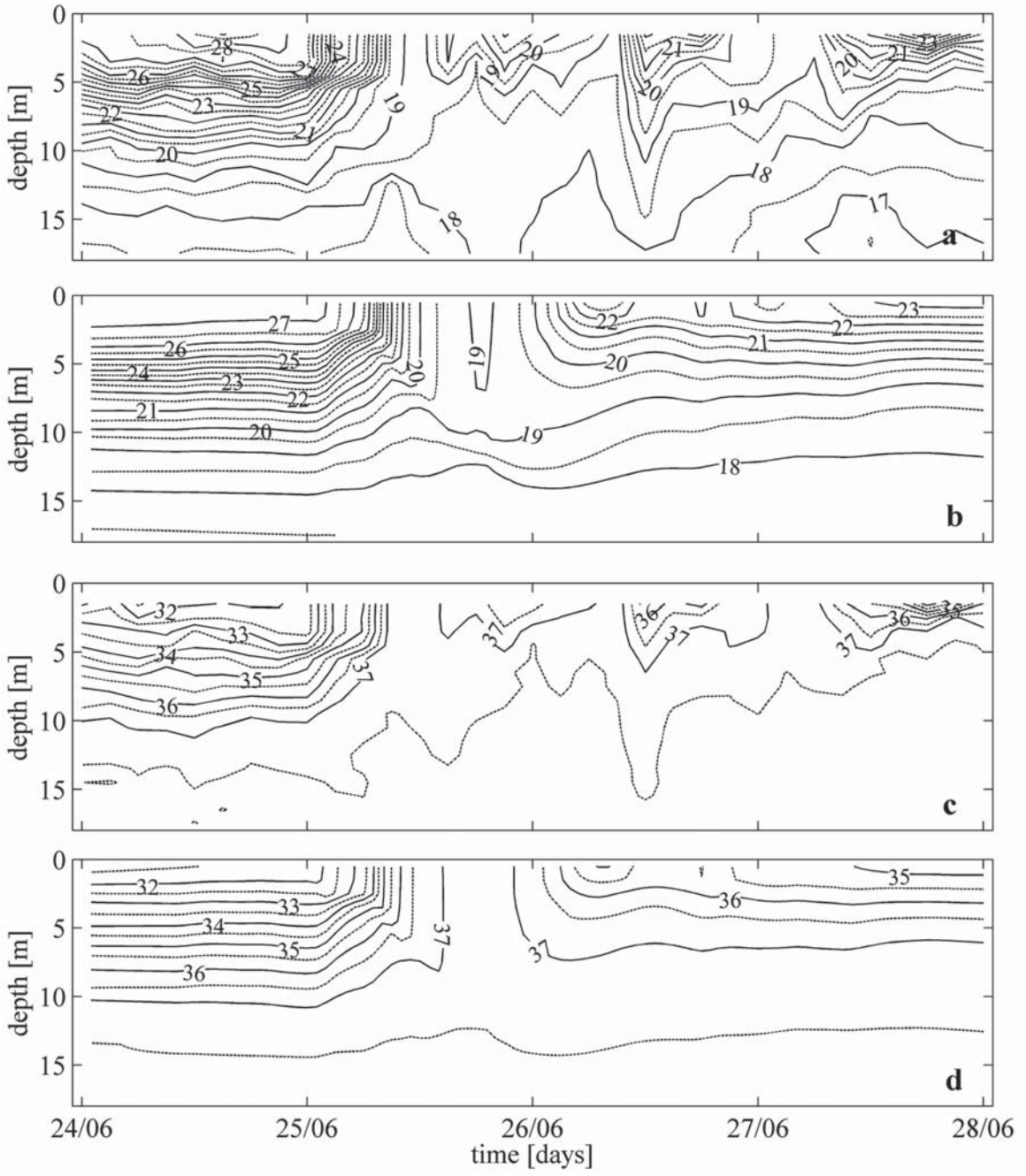

Fig. 6. Model validation: comparison between measured (a) and calculated (b) temperature vertical profiles and between measured (c) and calculated (d) salinity vertical profiles. Experimental data are collected by the MAMBO buoy vertical CTD profiler. The model does not take into account surface heating and cooling because it presently runs in adiabatic conditions. However, the upwelling event (00:00 – 12:00 of 25 June) induced by the bora wind is clearly reproduced. The surface recirculation of fresher water (35 psu) in the second half of 27 June is also caught by the model. NOTE: there are no buoy data for depths down to 1.0 – 1.5 m

the bora event (on 25 June, around 00:00) to the moment in which the satellite image was taken (26 June, 04:11), the averaged total heat flux is -130 Wm^{-2}. The bathymetry in the area ranges from 0 m to 15 m. If we consider the classic thermodynamic relationship:

$$Q = mc\,\Delta T$$

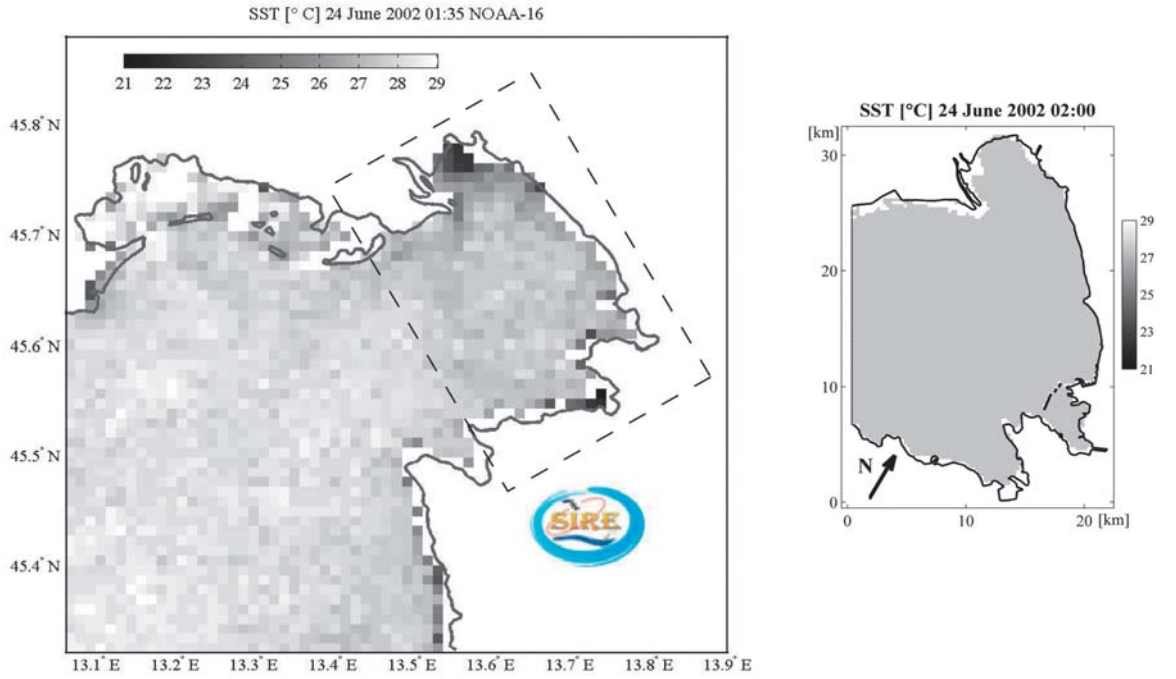

Fig. 7. Satellite image of the sea surface temperture (SST, [°C]) of a small portion of the northern Adriatic Sea including the GoT (left picture) and model result (right picture) at 01:35 and 02:00 of 24 June 2002, respectively. The satellite data are received and processed by the SIRE (Remote Sensing Group – SIstemi REmoti) group (OGS). SST is almost uniform in both plots even if the remotely sensed temperature values range from a minimum of 21 °C to a maximum of 29 °C. Since the model output is produced every hour, there is a time lag (25 minutes) between the images

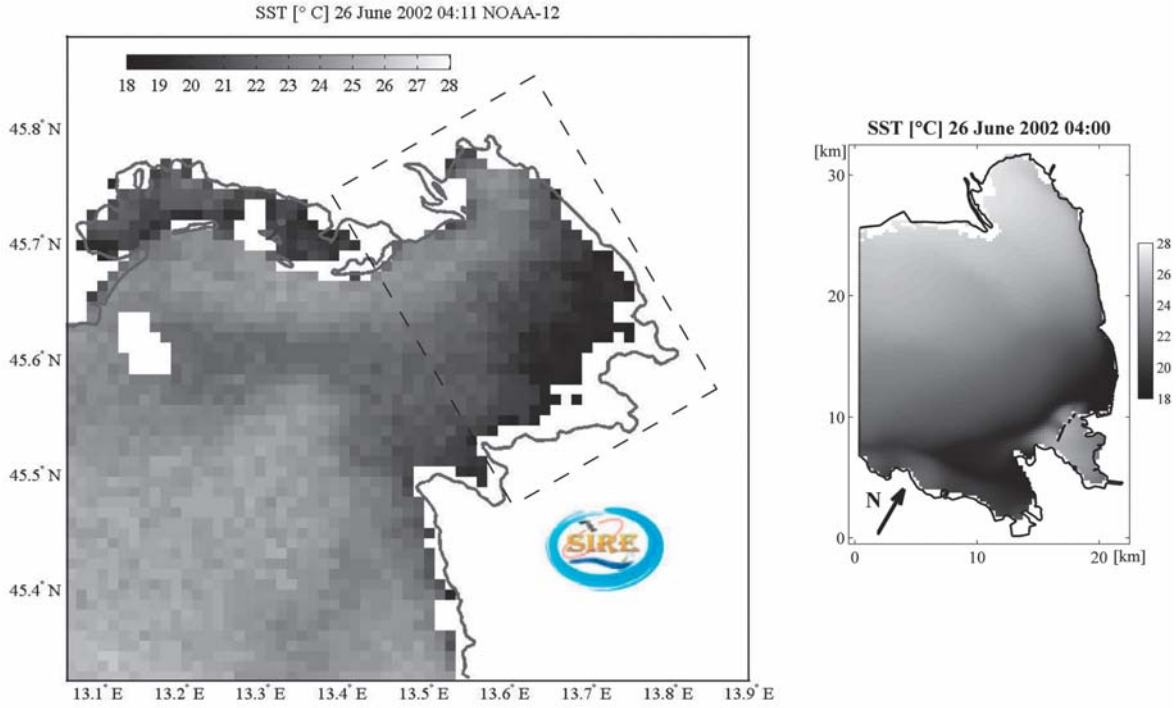

Fig. 8. Same plots as in Fig. 7, at 4:11 and 04:00 of 26 June 2002, respectively [°C]. The upwelling pattern on the south-eastern area of the basin is evident. The overall structure of the temperature field calculated by the model is similar to the one reproduced by the satellite image, with the major discrepancies in the north-western area and in the Bay of Panzano

where Q is the total heat [J], m the water mass [kg], c the heat capacity of the fluid [$Jkg^{-1}ºC^{-1}$] and ΔT the temperature variation [ºC], we maintain that we can achieve a temperature loss up to 3 ºC in the shallowest areas (1 m deep). On the other hand, where the bathymetry is deeper than 10-15 m (majority of the domain), the depth averaged effect of heat fluxes on the water column is much less ($\Delta T \geq 0.2 \div 0.3$ ºC).

It must be pointed out that the simulation forced with stronger wind (wind speed increased by 30%, run 7, Table 1, results not shown) gives SST values closer to the satellite data. In fact, stronger wind stress causes deeper mixing of the upper layer where surface warm water is mixed with larger quantities of intermediate colder water, hence the resulting overall surface temperature is lower. Although this configuration produces greater disagreement with the vertical temperature and salinity profiles near the MAMBO buoy site (sheltered from the wind), it is a sign of wind spatial non-homogeneity.

Description of model results

The simulations obtained with the realistic configuration for the June 2002 event show that an energetic circulation takes place only when bora starts to blow. Three layers can be identified: an uppermost (down to 5 m depth), an intermediate (5-13 m) and a deep (13 m-bottom) layer. Fig. 9 shows the current field evolution every 8 hours for the day of maximum wind stress (25/06/02, Fig. 2a). The plots in the first row show that the wind is too weak to induce a visible circulation in the basin. Eight hours later, velocity at the surface tends to have a negative (exiting) zonal component on both the northern and the southern side of the Gulf (Fig. 9 d). Veering of velocity in the center of the basin is roughly consistent, although smaller than that predicted by the EKMAN theory. This result was also obtained by MALAČIČ & PETELIN (2006) for the simulation of winter circulation (bora wind) using the Princeton Ocean Model (POM). In the proximity of the coastal areas, current direction is aligned with wind stress. As discussed for the real domain, ideal wind forcing case study (run 5) boundary effects and a time-dependent EKMAN solution in upwelling areas explain this anomaly. In the northernmost area (the Bay of Panzano) the shoaling of the bathymetry severely weakens the wind driven circulation. At 10 m depth (Fig. 9 e), the dynamics look quite different: the direct influence of the wind is lost and the incoming flux is basically induced by the recirculation due to the upwelling along the eastern coast. The horizontal divergence of velocity near the coastline in this area implies, because of continuity, the presence of an important vertical flux.

The dynamic balance of wind driven transport is even more evident in depth (Fig. 9f). In the bottom layer (15 m), the inflow of bottom water reaches its maximum velocity.

After sixteen hours, the velocity in the upper layer assumes the same pattern of Fig. 9 d, but the kinetic energy is lower. In the intermediate layer (Fig. 9h) there is also a substantial reduction both in average and maximum velocities and the direction of the current is oriented towards the NE. There is still an incoming flow into the bays of Muggia and Koper. The bottom circulation again compensates for the outgoing flow of the upper layer. The three-layer dynamics are now well established. In the last eight hours of 25/06 the wind forcing decreases and its direction is roughly SE. One day after the beginning of the bora event, the currents are decoupled from the wind stress (Fig. 9l). In particular, a southward surface current originates from the sea surface set-up, which is no longer sustained by the wind stress. The bottom incoming flux through the Bay of Muggia and the Bay of Koper is stopped (Fig. 9m, n).

Fig. 10 shows the temperature structure at the same levels (2, 10 and 15 m depth) and at the same timesteps as Fig. 9. The initial temperature is horizontally uniform, so any deviation is a signature of a vertical dynamic process. Fig. 10 (a, b and c) shows the thermal conditions before the onset of the bora event: horizontal uniformity at the surface and weak horizontal gradients (less than $0.02°Ckm^{-1}$) in the intermediate and bottom layers. The horizontal homogeneity of SST is also clearly indicated by the satellite images (e.g.: Fig. 7). After eight hours, a strong

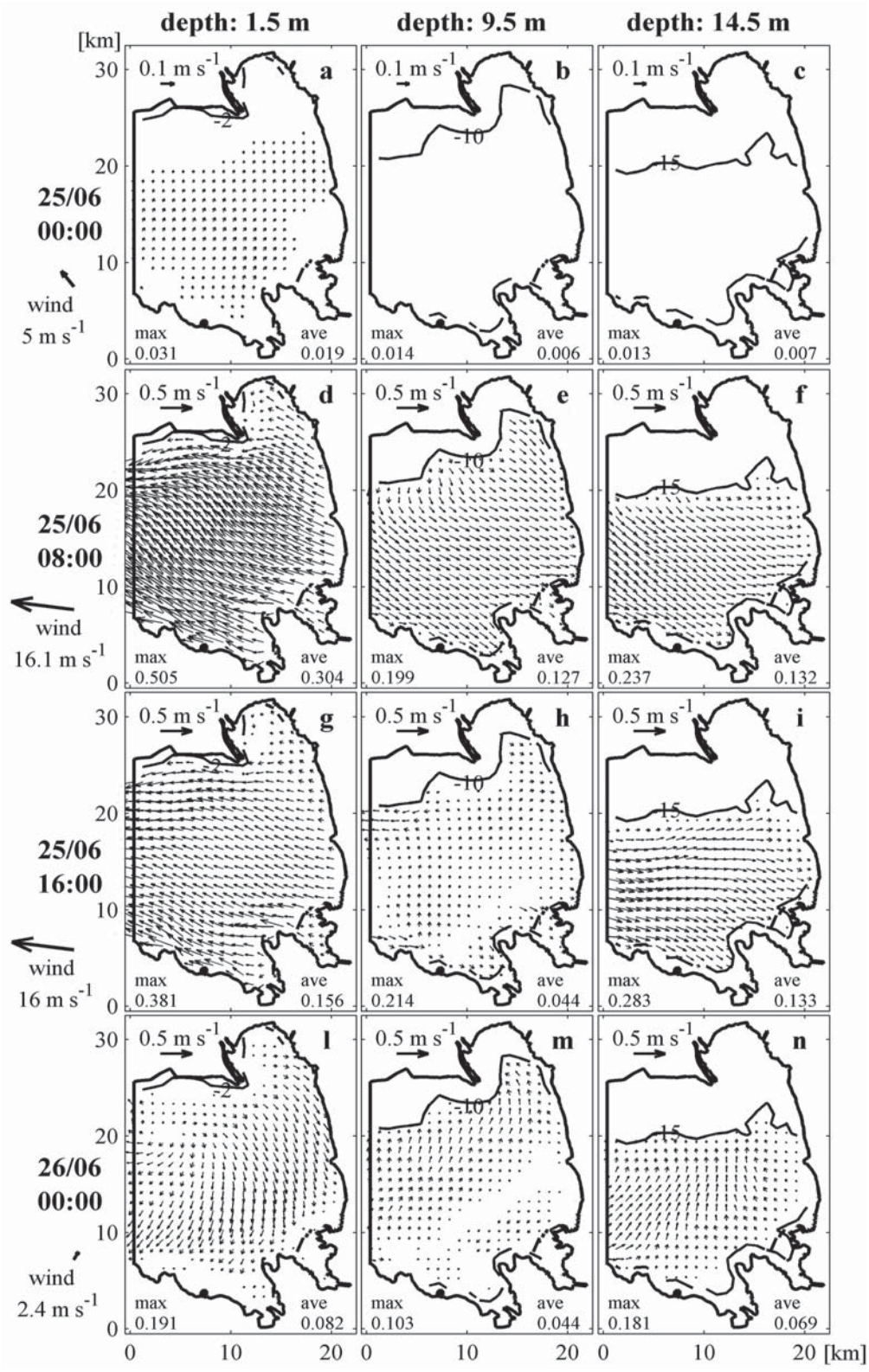

Fig. 9. Horizontal sections of velocity [ms^{-1}]: three levels (2, 10, 15 m) at four snapshots (00:00, 08:00, 16:00, 24:00 of 25 June 2002). In every sketch the maximum and the average velocity are indicated. The figure (expecially at 08:00) shows the influence of the bora wind on surface circulation (d): warm water flows outside the domain. Conversely, an inshore current of deep cold water (e and f) is flowing in the bottom layer, ensuring mass conservation

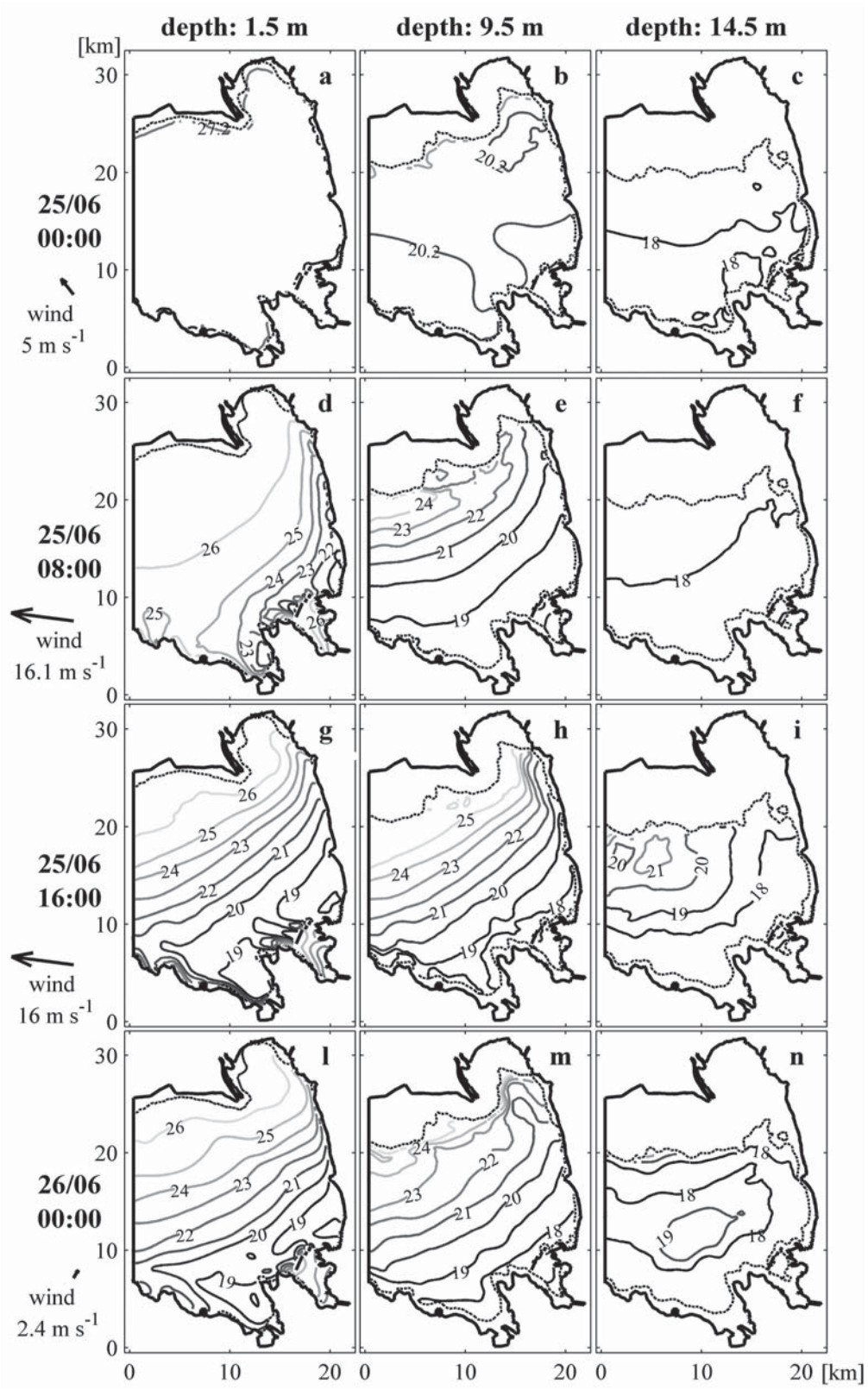

Fig. 10. Horizontal sections of temperature [°C]: three levels (2, 10, 15 m) at four snapshots (00:00, 08:00, 16:00, 24:00 of 25 June 2002). The bora event breaks the initial stable horizontal stratification after 8 hours. The upwelling temperature structure remains almost unchanged for one day (see, as a proof, the satellite image: Fig. 8)

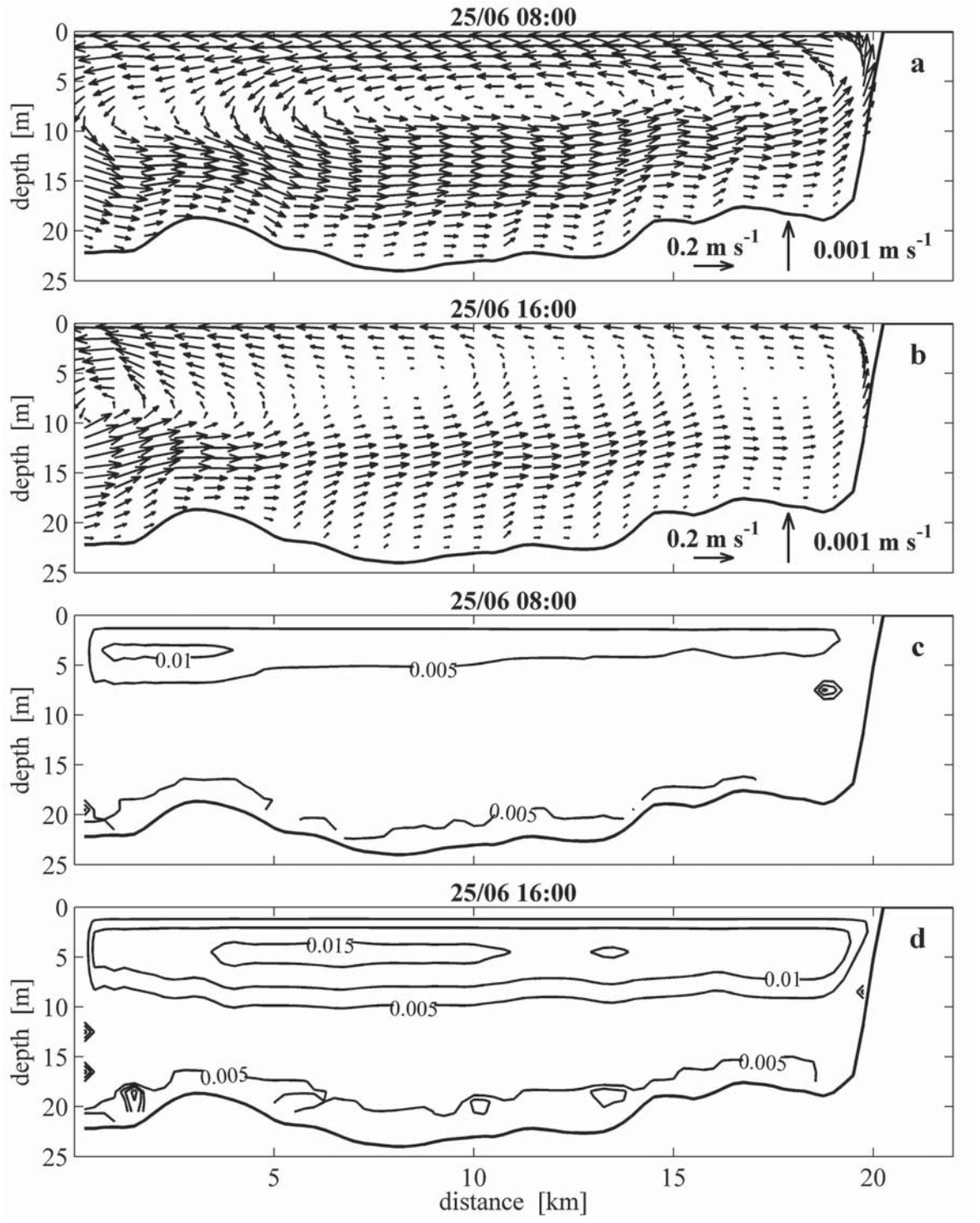

Fig. 11. Vertical sections of zonal, and vertical components of velocity ([ms^{-1}], plot a and b; the horizontal and vertical scales are different) and of the vertical eddy viscosity coefficient ([m^{2}s^{-1}], plot c and d) at 08:00 and 16:00 of 25 June 2002. The section is indicated in Fig. 1. There is a confined upwelling region along the eastern coast of the basin. The increase of the eddy viscosity coefficient near the surface and the growth of a bottom turbulent boundary layer are shown. The velocity anomalies (downward fluxes) near the western edge of the domain are due to the limitations of the ORLANSKI radiation condition which has been applied to the open boundary. Note that the KPP turbulent mixing parameterization does not take into account the effect of surface wave breaking

horizontal temperature gradient induced by the vertical dynamics is established throughout the basin. The maximum surface temperature (Fig. 10d) is almost the same as in the previous snapshot. Conversely, the temperature maxima in the intermediate layer is much higher than before (Fig. 10e). Minimum temperature values (<19 °C) are located in the southeastern corner of the basin, and are connected to the wind driven coastal upwelling. After sixteen hours, the thermal structure replicates the previous one, with a substantial cooling of the upper layer (Fig. 10g) and a warming of the intermediate and bottom layers. After one day, the horizontal gradient of temperature is still present (Fig. 10l). A smoothing of the thermal patterns is evident in the two deeper layers (Fig. 10m, n).

Velocity on a vertical section crossing the Gulf of Trieste is shown in Fig. 11a and b (see Fig. 1 for the position of the transect). In this case, two snapshots are compared: the first (Fig. 11a) represents the u and w components of the velocity at 08:00 of 25 June while the second (Fig. 11b) shows the same section 8 hours later. The presence of three layer dynamics is evident in both snapshots. An outgoing flux is almost homegeneously distributed in the first 5 m while an incoming flux influences the deepest part of the basin (below 7 m). The boundary effects due to wall friction are present only in the proximity of the bottom. An intermediate, less energetic layer decouples the upper layer from the bottom one. Coastal upwelling takes place on the eastern side of the basin.

Model results also agree with the theoretical analysis of coastal upwelling, both in the transient and in the steady case. The upwelling structure should have a length scale equal to a, the first Rossby internal radius of deformation (KANTHA & CLAYSON, 2000), which is given by:

$$a = \sqrt{g'H} \,/\, f$$

where g' is the reduced gravity, H is the average depth and f is the Coriolis parameter. In this case $g' = 10^{-2}$ ms^{-2}, H = 20 m and $f = 10^{-4}$ s^{-1} which give $a \cong 4.5$ km. The horizontal sections of temperature given by the model and the satellite image of SST show that the oucropping cold water (around 20 °C) structure is characterized by a similar horizontal length scale.

If we impose a stronger wind forcing (wind speed increased by 30%, results not shown), the model output is quite different. More energetic horizontal velocity fields, with the formation and intensification of a cyclonic structure, are present. The temperature stratification is eroded faster and deeper than in the previous case: this leads to lower SST values because surface warm water is mixed with a larger quantity of intermediate and deep cold water. Similar behaviour can be observed for the velocity and the eddy viscosity coefficient. An overall more energetic flow with a deeper EKMAN turbulent layer is present. Some hours after the onset of the bora wind the situation is almost analogous to the previous case but with a stronger incoming bottom flow. The eddy viscosity coefficient also indicates the presence of stronger turbulent motions both in the surface and the bottom layers.

CONCLUSIONS

The importance of a correct parametrization of vertical turbulent processes is investigated by analyzing the EKMAN boundary layer with a state of the art numerical model. The influence of vertical thermohaline stratification is also studied.

Then attention is focused on the wind driven circulation in the Gulf of Trieste during summer. When strong bora events occur, the circulation is mainly governed by the EKMAN transport, which moves surface water masses offshore, towards the northern coast. Superficial outflow of warm water is balanced by an inflow of deep cold water. This circulation induces an upwelling of the deepest water masses along the south-eastern coast of the basin. Such a phenomenon can cause several enviromental problems if, for example, sewage waters (which are treated and discharged in such a way to

remain and disperse in the bottom layers) are involved in the process. Fairly good agreement with experimental observations, despite the approximations adopted, proves the reliability of the model. The next step in this research will be the implementation of a one-way nesting with the larger-scale model ACOAST-1.2 (following the model hierarchy adopted by the ADRICOSM project). The coupling with a high resolution LAM atmospheric model, the introduction of atmospheric heat fluxes and the modeling of the Isonzo River freshwater input will be introduced in the near future. These improvements will increase the model reliability.

ACKNOWLEDGEMENTS

This study was carried out within the ADRICOSM and MFSTEP international projects. The authors thank CINECA and Cristiano CALONACI for the precious informatics support; CNR-ISMAR and ARPA FVG-OSMER for the meteorological data; Davide DEPONTE and Dino VIEZZOLI (OGS) for the MAMBO buoy data. A special thanks goes to Giulio NOTARSTEFANO (SIRE group - OGS) for the satellite data processing.

REFERENCES

ACCERBONI, E. & B. MANCA. 1973. Storm surge forecasting in the Adriatic Sea by means of a two-dimensional hydrodynamical numerical model. Boll. Oceanol. Teor. Applic., 15 (57): 3-22.

CARMINATI, B., A. CRISE & R. MOSETTI. 1994. Transport and Spreading Model for an Oil Spill event in the Gulf of Trieste. In: E. Verri (Editor). Proceedings of 'EUROPROTECH', Udine, Italy, 6-8 May, pp. 271-285.

CAVALLINI, F. 1985. A three-dimensional numerical model of tidal circulation in the northern Adriatic Sea. Boll. Oceanol. Teor. Applic., 3: 205-218.

EKMAN, V. W. 1905. On the influence of the earth's rotation on ocean currents. Arkiv. Math. Astron. Phys., 2 (11): 1-52.

HUANG, N. E. 1979. On surface drift currents in the ocean. J. Fluid Mech., 91: 191-208.

HASSELMANN, K. 1970. Wave-driven inertial oscillations. Geophys. Astrophys. Fluid Dyn., 1: 463-502.

KANTHA, L. H. & C. A. CLAYSON. 2000. Numerical Models of Oceans and Oceanic Processes. Academic Press. San Diego, CA, Int. Geophysics Series, 66: 96-100.

LARGE, W. G. & S. POND. 1981. Open ocean flux measurements in moderate to strong winds. J. Phys. Oceanogr., 11: 324-336.

LARGE, W. G. & S. POND. 1982. Sensible and latent heat flux measurements over the ocean. J. Phys. Oceanogr., 12: 464-482.

LARGE, W. G., J. C. McWILLIAMS & C. S. DONEY. 1994. Oceanic vertical mixing: a review and a model with non local boundary layer parameterization. Rev. Geophys., 32: 363-403.

LONGO, R., F. RAICICH & R. MOSETTI. 1990. A numerical model of transport and diffusion of radionuclides in the Gulf of Trieste. Boll. Oceanol. Teor. Applic., 8 (1): 13-24.

MALAČIČ, V., D. VIEZZOLI & B. CUSHMAN-ROISIN. 2000. Tidal dynamics in the northern Adriatic Sea. J. Geophys. Res., 105 (26): 265-280.

MALAČIČ, V. & B. PETELIN. 2006. Numerical modeling of the winter circulation of the Gulf of Trieste (northern Adriatic). Acta Adriat., 47 (Suppl.): 207-217.

MARSHALL, J., A. ADCROFT, C. HILL, L. PERELMAN & C. HEISEY. 1997. A finite-volume, incompressible Navier Stokes model for studies of the ocean on parallel computers. J. Geophys. Res., 102: 5753-5766.

MARSHALL, J. & F. SCHOTT. 1999. Open-ocean convection: observations, theory and models. Rev. Geophys., 37: 1-64.

MOSETTI, F. & B. MANCA. 1972. Some methods of tidal analysis. Int. Hydrogr. Rev. 49 (2): 107-120.

NOTARSTEFANO, G., E. MAURI & P. M. POULAIN. 2004. Comparison analysis between bulk sea water temperature, as measured by drifters, and sea surface temperature derived by satellite measurements. Rel-I-22 OGA-11, OGS, Trieste, Italy, 22 pp.

OLIVO, P. 2002. Sulla circolazione del Golfo di Trieste e sua influenza sulla diffusione di inquinanti (On circulation in the Gulf of Trieste and its impact on pollutant distribution). Thesis, University of Trieste, 105 pp.

ORLANSKI, I. 1976. A simple boundary condition for unbounded hyperbolic flows. J. Computational Physics., 21: 251-269.

PICCO, P. 1991. Evaporation and heat exchanges between the sea and the atmosphere in the Gulf of Trieste during 1988. Il Nuovo Cimento, 14 C (4): 335-345.

QUERIN, S. 2002. Analisi teorico sperimentale dei processi convettivi in acque costiere: il Golfo di Trieste (Experimental-theoretical analysis of convective processes in coastal waters: The Gulf of Trieste). Thesis, University of Trieste, 90 pp.

SCHUDLICH, R. R. & J . F. PRICE. 1998. Observations of seasonal variation in the Ekman layer. J. Phys. Oceanogr., 28: 1187-1204.

STRAVISI, F. 2001. La Bora a Trieste (The bora wind in Trieste). Unione Meteorologica Friuli-Venezia Giulia, Atti I Conv., pp. 23-34.

WELLER, R. A., D. L. RUDNICK, C. C. ERIKSEN, K. L. PLOZIN, N. S. OAKEY, J. W. TOOLE, R. W. SCHMITT & R. T. POLLARD. 1991. Forced ocean response during the Frontal Air-Sea Interaction Experiment. J. Geophys. Res., 96: 8611-8638.

ZAVATARELLI, M. & N. PINARDI. 2003. The Adriatic Sea modeling system: a nested approach. Ann. Geophys., 21: 345-364.

Strujanje uzrokovano vjetrom u stratificiranom fluidu: numeričko istraživanje i primjena na Tršćanski zaljev u uvjetima jake bure

Alessandro CRISE [1*], Stefano QUERIN [1] i Vlado MALAČIČ [2]

[1] *Nacionalni institut za eksperimentalnu oceanografiju i geofiziku (OGS), Borgo Grotta Gigante, 42/C, 34010 Sgonico (Trst), Italija*

[2] *Nacionalni biološki institut, Centar za istraživanje mora, 6330 Piran, Slovenija*

**Kontakt adresa, e-mail: acrise@ogs.trieste.it*

SAŽETAK

U ovom se radu analizira strujanje u Tršćanskom zaljevu uzrokovano jakom burom u vertikalno stratificiranom slučaju. Preliminarna numerička analiza strujnog polja uzrokovanog vjetrom urađena je za idealizirani slučaj horizontalno neograničene domene. Zatim su numeričke simulacije primijenjene na Tršćanski zaljev upotrebivši realnu batimetriju i uz pretpostavku vertikalno stabilne stratifikacije. 25. lipnja 2002. godine najprije je primjenijen stacionaran vjetar, a zatim realistična situacija jake bure. Rezultati numeričke integracije pokazuju dobro slaganje s *in situ* i daljinskim mjerenjima. Posebna je pažnja poklonjena intenzitetu obalnog "upwellinga" i njegovoj postojanosti. Rezultati ukazuju da su vertikalno miješanje i "upwelling" odgovorni za strujanje u bazenu. Bura uzrokuje EKMANOV transport i odnosi slatku vodu prema sredini zaljeva, te uzrokuje formiranje pridnene struje ka obali. Istovremeno vertikalno miješanje slabi vertikalnu stabilnost vodenog stupca. Površinska struja od obale prema sredini zaljeva uzrokuje nagib razine mora od sjeverne obale ka jugu. Kada prestane bura nagib razine mora se više ne može održati i javlja se površinska struja suprotnog smjera. U ovom je radu također istraživana osjetljivost numeričkih rješenja na utjecaj vjetra. Ovi su procesi važni za širenje otpadnih tvari kao i za eventualnu pojavu anoksije u pridnenom sloju zaljeva.

Ključne riječi: strujanje uzrokovano vjetrom, bura, EKMANOV sloj, upwelling, miješanje